MHD natural convective Casson Fluid Flow over an Oscillating vertical Plate under the influence of thermal diffusion

Vasa Raghu, Research Scholar (PP.MAT.0138), Rayalaseema University, Kurnool, AP, INIDA, sairaghugss9@gmail.com

G S S Raju, Professor, Department of Mathematics, JNT College of Engineering, Pulivendula, AP, INDIA. rajugss@gmail.com

Avula Golla Vijaya Kumar, Senior Assistant Professor, Department of Mathematics, SAS, VIT,Vellore, TN, INDIA. vijayakumarag@vit.ac.in

Abstract: In this work, the heat and mass transfer effects on unsteady MHD free convective Casson fluid flow past an oscillating semi-infinite vertical plate in the presence of porous medium with a heat source under the influence of uniform transverse applied magnetic field is considered. A general exact solution of the dimensionless governing partial differential equations is obtained by Laplace transform technique without any restriction. The numerical values of Casson fluid velocity, temperature, species concentration are displayed graphically and also discussed the effects of various flow parameters such as the rate of heat transfer and the rate of mass transfer at the surface of the wall. Casson parameter is inversely proportional to the yield stress and it is observed that for the large value of Casson parameter, the fluid is close to the Newtonian fluid where the velocity is less than the non-Newtonian fluid. It has been found that when the heat source parameter increases the species concentration profiles decreased.

Keywords — ***Casson fluid, heat source, heat and mass transfer, magnetic field , porous medium, Soret effect***

I. INTRODUCTION

Casson fluid model was introduced by Casson [5] for the prediction of the flow behavior of pigment-oil suspension. So for the flow, the shear stress magnetic of Casson fluid needs to exceed the yield shear stress, or else the fluid behaves as a rigid body. This kind of fluids can be marked as a purely viscous fluid with high viscosity. Casson model is based on a structural model of the interactive behavior of solid and liquid phases of two-phase suspensions. Examples are honey, jelly, sauce, tomato, soup and concentrated fruit juice. Human blood can also be treated as Casson fluid due to the presence of several substances such as fibrinogen, protein, globulin in aqueous base plasma and human red blood cell. The effects of thermophoresis and some thermo-physical properties on free convective heat and mass transfer of non-Darcian MHD flow over vertical porous plate with n^{th} order of chemical reaction in the presence of suction, plastic dynamic viscosity of the non-Newtonian fluid together with thermal conductivity are assumed to vary as a linear function of temperature studied by Animasaun [1]. Several numerical studies of Casson fluid flow with different effects can be found in [7-13, 19, 21-23 and 26]. The Casson fluid model is used to characterize the non- Newtonian fluid behavior. In the earlier studies on Casson fluid, Boyd et al. [4] discussed the steady and oscillatory flows of blood by taking into account Casson fluid. Bhattacharyya [2] constructed the boundary layer stagnation-point flow of Casson fluid and heat transfer towards a shrinking/stretching sheet. Exact solution for boundary layer flow of Casson fluid over a permeable shrinking/stretching sheet is studied by Bhattacharyya et al. [3]. Vajravelu and Mukhopadhyay [27] considered diffusion of chemically reactive species in Casson fluid flow over an unsteady permeable stretching surface. The various effects of the Casson fluid flow in a pipe filled with a homogeneous porous medium have been examined by Dash et al. [6]. The MHD flow of a Casson fluid over an exponentially shrinking sheet was addressed by Nadeem et al. [18]. The effects of unsteady boundary layer flow of a Casson fluid due to an impulsively started moving flat plate have been studied by Mustafa et al. [16]. The diffusion of chemically reactive species in Casson fluid flow over an unsteady permeable stretching surface has been investigated by Mukhopadhyay and Vajravelu [14]. Thermal diffusion and radiation effects on unsteady free convection flow in the presence of magnetic field fixed relative to the fluid or to

 DOI : 10.35291/2454-9150.2019.0483

the plate was examined by Rushi Kumar et al. [20]. Reddy et al. [24] studied the thermal diffusion and chemical reaction effects on an unsteady MHD dusty fluid with various physical properties. Recently Reddy et al. [25] examined the influence of chemical reaction, radiation, and rotation on MHD nanofluid flow past a permeable flat plate in a porous medium. In this study, they found that an increase in the convective parameter increases the temperature profiles of the flow. Veerareddy et.al [28] investigated heat and mass transfer effects on unsteady MHD Casson fluid past a vertical plate in the presence of porous medium.

In this work, we extend the work of Khalid et al. [11] in which the heat source term is taken into the energy equation and species concentration equations are also introduced. The motivation of the present study is to bring out the effects of heat source and Soret effect on Casson fluid flow past an oscillating semi-infinite vertical plate in the presence of a porous medium. The dimensionless governing equations are solved using the Laplace transform technique. In this work, we investigate the effect of varying physical parameter, Casson, Schmidt and Prandtl numbers on velocity, temperature and species concentration profiles with the depiction of graphical and the physical aspects are discussed in detail.

II. MATHEMATICAL ANALYSIS

Consider heat and mass transfer effects on unsteady MHD free convective Casson fluid flow past an oscillating semi-infinite vertical plate in the presence of porous medium with a heat source under the influence of uniform transverse magnetic field. The x' -axis is taken along the vertical plate in the upward direction and y' - axis is normal to it. A uniform magnetic field of strength B_0 is applied normal to the fluid flow direction. Initially, it is assumed that at the time $t' \le 0$, both the plate and surrounding fluid are at the same temperature and concentration in a stationary condition for all the points in the entire flow region $y' \ge 0$. At the time $t' > 0$, the plate is given an oscillatory motion in the vertical direction against a gravitational field with velocity $u' = u_0 \cos(\omega' t')$. At the same time, the temperature of the plate is raised to T_w' and the mass levels near the plate are raised to C_w'. The fluid is assumed to be gray emitting and absorbing radiation but non- scattering medium. It also assumed that the applied magnetic field is uniform and that the magnetic Reynolds number is small so that the induced magnetic field is neglected. All the fluid properties are assumed to be constant except the influence of the density variation with temperature in the body force term. Electric field and dissipation effects are neglected. The constitutive equation for the Casson fluid can be written as Mustafa et al. [17]

$$\tau_{ij} = \begin{cases} 2\left(\mu_B + \dfrac{P_y}{\sqrt{2\pi}}\right)e_{ij} & \pi > \pi_c \\ 2\left(\mu_B + \dfrac{P_y}{\sqrt{2\pi_c}}\right)e_{ij} & \pi < \pi_c \end{cases},$$

Where $\pi = e_{ij}, e_{ij}$ and e_{ij} is the (i, j)th component of the deformation rate, π is the product of the component of deformation rate with itself, π_c is a critical value of this product based on the non-Newtonian model, μ_B is the plastic dynamic viscosity of the non-Newtonian fluid and P_y is yield stress of fluid.

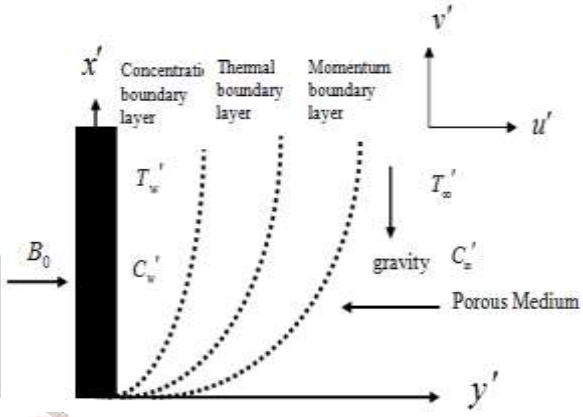

Fig. 1 Physical coordinate system

Based on these assumptions, the fluid flow can be represented by the following system of governing equations

$$\frac{\partial u'}{\partial t'} = \nu\left(1+\frac{1}{\gamma}\right)\frac{\partial^2 u'}{\partial y'^2} + g\beta\left(T'-T_\infty'\right) + g\beta^*\left(C'-C_\infty'\right) - \frac{\sigma B_0^2 u'}{\rho} - \nu\frac{u'}{K'} \quad (1)$$

$$\rho c_p \frac{\partial T'}{\partial t'} = k\frac{\partial^2 T'}{\partial y'^2} - \frac{\partial q_r}{\partial y'} - Q'\left(T'-T_\infty'\right) \quad (2)$$

$$\frac{\partial C'}{\partial t'} = D\frac{\partial^2 C'}{\partial y'^2} + D_1\frac{\partial^2 T'}{\partial y'^2} - k'\left(C'-C_\infty'\right) \quad (3)$$

With the following initial and boundary conditions

$t' \le 0 : u' = 0, \quad T' = T_\infty', \quad C' = C_\infty'$, for all y'

$t' > 0 : u' = u_0\cos(\omega' t'), \quad T' = T_w', \quad C' = C_w'$ at $y' = 0$

$u' \to 0, \quad T' \to T_\infty', \quad C' \to C_\infty'$, as $y' \to \infty$

On introducing the following non-dimensional quantities

$$u = \frac{u'}{u_0},\ t = \frac{t'u_0^2}{\nu},\ y = \frac{y'u_0}{\nu},\ \theta = \frac{T'-T_\infty'}{T_w'-T_\infty'},\ C = \frac{C'-C_\infty'}{C_w'-C_\infty'},$$

$$Gr = \frac{g\beta\nu\left(T_w'-T_\infty'\right)}{u_0^3},\ Gm = \frac{g\beta^*\nu\left(C_w'-C_\infty'\right)}{u_0^3},\ \Pr = \frac{\nu\rho C_p}{k},\ \omega = \frac{\omega'\nu}{u_0^2}$$

$$S_0 = \frac{D_1\left(T_w'-T_\infty'\right)}{\nu\left(C_w'-C_\infty'\right)},\ M = \frac{\sigma B_0^2\nu}{\rho u_0^2},\ Q = \frac{Q'\nu}{\rho C_p u_0^2},\ Sc = \frac{\nu}{D},\ K = \frac{ku_0^2}{\phi\nu^2} \quad (4)$$

where $A = \dfrac{u_0^2}{\nu}$ the local radiant, the optically thick radiation limit is considered in the present analysis. The radiative heat flux for an optically thick fluid can be found from Rosseland approximation and its formula is derived from

 DOI : 10.35291/2454-9150.2019.0483

the diffusion concept of radiative heat transfer in the following way:

$$q_r = \frac{-4\sigma}{3k*}\frac{\partial T'^4}{\partial y'} \quad (5)$$

$$T'^4 \cong 4T'^3_\infty T' - 3T'^4_\infty \quad (6)$$

From Eqs. (5) and (6), Eq. (2) reduces to

$$\rho c_p \frac{\partial T'}{\partial t'} = k\frac{\partial^2 T'}{\partial t'^2} + \frac{16\sigma T'^3_\infty}{3k^*}\frac{\partial^2 T'}{\partial y'^2} \quad (7)$$

We get the following governing equations which are dimensionless.

$$\frac{\partial u}{\partial t} = \left(1+\frac{1}{\gamma}\right)\frac{\partial^2 u}{\partial y^2} + Gr\theta + GmC - \left(M+\frac{1}{K}\right)u \quad (8)$$

$$\frac{\partial \theta}{\partial t} = \left(\frac{3R+4}{3R\,\mathrm{Pr}}\right)\frac{\partial^2 \theta}{\partial y^2} - \frac{Q}{\mathrm{Pr}}\theta \quad (9)$$

$$\frac{\partial C}{\partial t} = \frac{1}{Sc}\frac{\partial^2 C}{\partial y^2} + S_0\frac{\partial^2 \theta}{\partial y^2} - kC \quad (10)$$

The initial and boundary conditions in dimensionless form are as follows:

$$t \le 0 : u = 0, \quad \theta = 0, \quad C = 0 \text{ for all } y$$

$$t > 0 : u = \cos(\omega t), \quad \theta = 1, \quad C = 1 \text{ at } y = 0$$

$$u \to 0, \quad \theta \to 0, \quad C \to 0 \text{ as } y \to \infty \quad (11)$$

The appeared physical parameters are defined in the nomenclature. The dimensionless governing equations from (8) to (10), subject to the boundary conditions (11) are solved by usual Laplace transform technique and the solutions are expressed in terms of exponential and complementary error functions

$$\theta(y,t) = \frac{1}{\alpha}\left[\begin{array}{l}\left(\frac{t\alpha}{2}+\frac{y\,\mathrm{Pr}}{4\sqrt{b_0}}\right)\exp\left(y\sqrt{b_0}\right)erfc\left(\frac{y\sqrt{\mathrm{Pr}}}{2\sqrt{\alpha t}}+\sqrt{\frac{Qt}{\mathrm{Pr}}}\right)\\ +\left(\frac{t\alpha}{2}-\frac{y\,\mathrm{Pr}}{4\sqrt{b_0}}\right)\exp\left(-y\sqrt{b_0}\right)erfc\left(\frac{y\sqrt{\mathrm{Pr}}}{2\sqrt{\alpha t}}-\sqrt{\frac{Qt}{\mathrm{Pr}}}\right)\end{array}\right] \quad (12)$$

$$C(y,t) = (1+b_4)\left[\begin{array}{l}\left(\frac{t}{2}+\frac{y\sqrt{Sc}}{4\sqrt{k}}\right)\exp\left(y\sqrt{kSc}\right)erfc\left(\frac{y\sqrt{Sc}}{2\sqrt{t}}+\sqrt{kt}\right)\\ +\left(\frac{t}{2}-\frac{y\sqrt{Sc}}{4\sqrt{k}}\right)\exp\left(-y\sqrt{kSc}\right)erfc\left(\frac{y\sqrt{Sc}}{2\sqrt{t}}-\sqrt{kt}\right)\end{array}\right]$$

$$+\frac{(b_5+b_6)}{2}\left[\begin{array}{l}\exp\left(y\sqrt{kSc}\right)erfc\left(\frac{y\sqrt{Sc}}{2\sqrt{t}}+\sqrt{kt}\right)\\ +\exp\left(-y\sqrt{kSc}\right)erfc\left(\frac{y\sqrt{Sc}}{2\sqrt{t}}-\sqrt{kt}\right)\end{array}\right]$$

$$+\frac{(-b_5-b_6)\,e^{(b_2 t)}}{2}\left[\begin{array}{l}\exp\left(y\sqrt{(k+b_2)Sc}\right)erfc\left(\frac{y\sqrt{Sc}}{2\sqrt{t}}+\sqrt{(k+b_2)t}\right)\\ +\exp\left(-y\sqrt{(k+b_2)Sc}\right)erfc\left(\frac{y\sqrt{Sc}}{2\sqrt{t}}-\sqrt{(k+b_2)t}\right)\end{array}\right]$$

$$-\frac{b_4}{\alpha}\left[\begin{array}{l}\left(\frac{t\alpha}{2}+\frac{y\,\mathrm{Pr}}{4\sqrt{b_0}}\right)\exp\left(y\sqrt{b_0}\right)erfc\left(\frac{y\sqrt{\mathrm{Pr}}}{2\sqrt{\alpha t}}+\sqrt{\frac{Qt}{\mathrm{Pr}}}\right)\\ +\left(\frac{t\alpha}{2}-\frac{y\,\mathrm{Pr}}{4\sqrt{b_0}}\right)\exp\left(-y\sqrt{b_0}\right)erfc\left(\frac{y\sqrt{\mathrm{Pr}}}{2\sqrt{\alpha t}}-\sqrt{\frac{Qt}{\mathrm{Pr}}}\right)\end{array}\right]$$

$$+\frac{(-b_5-b_6)}{2}\left[\begin{array}{l}\exp\left(y\sqrt{b_0}\right)erfc\left(\frac{y\sqrt{\mathrm{Pr}}}{2\sqrt{\alpha t}}+\sqrt{\frac{Qt}{\mathrm{Pr}}}\right)\\ +\exp\left(-y\sqrt{b_0}\right)erfc\left(\frac{y\sqrt{\mathrm{Pr}}}{2\sqrt{\alpha t}}-\sqrt{\frac{Qt}{\mathrm{Pr}}}\right)\end{array}\right]$$

$$+\frac{(b_5+b_6)\,e^{(b_2 t)}}{2}\left[\begin{array}{l}\exp\left(y\sqrt{b}\right)erfc\left(\frac{y\sqrt{\mathrm{Pr}}}{2\sqrt{\alpha t}}+\sqrt{\frac{bt}{\mathrm{Pr}}}\right)\\ +\exp\left(-y\sqrt{b}\right)erfc\left(\frac{y\sqrt{\mathrm{Pr}}}{2\sqrt{t}}-\sqrt{\frac{bt}{\mathrm{Pr}}}\right)\end{array}\right] \quad (13)$$

$$u(y,t) = \frac{e^{(a_0 t)}}{2}\left[\begin{array}{l}\exp\left(y\sqrt{a_2}\right)erfc\left(\frac{y}{2\sqrt{Bt}}+\sqrt{a_2 t}\right)\\ +\exp\left(-y\sqrt{a_2}\right)erfc\left(\frac{y}{2\sqrt{Bt}}-\sqrt{a_2 t}\right)\end{array}\right]$$

$$+\frac{A_0}{2}\left[\begin{array}{l}\exp\left(y\sqrt{a_1}\right)erfc\left(\frac{y}{2\sqrt{Bt}}+\sqrt{a_1 t}\right)\\ +\exp\left(-y\sqrt{a_1}\right)erfc\left(\frac{y}{2\sqrt{Bt}}-\sqrt{a_1 t}\right)\end{array}\right]$$

$$+\frac{A_1}{2B}\left[\begin{array}{l}\left(\frac{tB}{2}+\frac{y}{4\sqrt{a_1}}\right)\exp\left(y\sqrt{a_1}\right)erfc\left(\frac{y}{2\sqrt{Bt}}+\sqrt{a_1 t}\right)\\ +\left(\frac{tB}{2}-\frac{y}{4\sqrt{a_1}}\right)\exp\left(-y\sqrt{a_1}\right)erfc\left(\frac{y}{2\sqrt{Bt}}-\sqrt{a_1 t}\right)\end{array}\right]$$

$$+\frac{A_2\,e^{(-b_8 t)}}{2}\left[\begin{array}{l}\exp\left(y\sqrt{a_3}\right)erfc\left(\frac{y}{2\sqrt{Bt}}+\sqrt{a_3 t}\right)\\ +\exp\left(-y\sqrt{a_3}\right)erfc\left(\frac{y}{2\sqrt{Bt}}-\sqrt{a_3 t}\right)\end{array}\right]$$

$$+\frac{A_3\,e^{(-b_{10} t)}}{2}\left[\begin{array}{l}\exp\left(y\sqrt{a_4}\right)erfc\left(\frac{y}{2\sqrt{Bt}}+\sqrt{a_4 t}\right)\\ +\exp\left(-y\sqrt{a_4}\right)erfc\left(\frac{y}{2\sqrt{Bt}}-\sqrt{a_4 t}\right)\end{array}\right]$$

$$+\frac{A_4\,e^{(b_2 t)}}{2}\left[\begin{array}{l}\exp\left(y\sqrt{a_5}\right)erfc\left(\frac{y}{2\sqrt{Bt}}+\sqrt{a_5 t}\right)\\ +\exp\left(-y\sqrt{a_5}\right)erfc\left(\frac{y}{2\sqrt{Bt}}-\sqrt{a_5 t}\right)\end{array}\right]$$

$$+\frac{A_5}{2}\left[\begin{array}{l}\exp\left(y\sqrt{b_0}\right)erfc\left(\frac{y\sqrt{\mathrm{Pr}}}{2\sqrt{\alpha t}}+\sqrt{\frac{Qt}{\mathrm{Pr}}}\right)\\ +\exp\left(-y\sqrt{b_0}\right)erfc\left(\frac{y\sqrt{\mathrm{Pr}}}{2\sqrt{\alpha t}}-\sqrt{\frac{Qt}{\mathrm{Pr}}}\right)\end{array}\right]$$

$$+\frac{A_6}{\alpha}\left[\begin{array}{l}\left(\frac{t\alpha}{2}+\frac{y\,\mathrm{Pr}}{4\sqrt{b_0}}\right)\exp\left(y\sqrt{b_0}\right)erfc\left(\frac{y\sqrt{\mathrm{Pr}}}{2\sqrt{\alpha t}}+\sqrt{\frac{Qt}{\mathrm{Pr}}}\right)\\ +\left(\frac{t\alpha}{2}-\frac{y\,\mathrm{Pr}}{4\sqrt{b_0}}\right)\exp\left(-y\sqrt{b_0}\right)erfc\left(\frac{y\sqrt{\mathrm{Pr}}}{2\sqrt{\alpha t}}-\sqrt{\frac{t}{\mathrm{Pr}}}\right)\end{array}\right]$$

$$+\frac{A_7\,e^{(-b_8 t)}}{2}\left[\begin{array}{l}\exp\left(y\sqrt{a_6}\right)erfc\left(\frac{y\sqrt{\mathrm{Pr}}}{2\sqrt{t}}+\sqrt{\frac{a_6 t}{\mathrm{Pr}}}\right)\\ +\exp\left(-y\sqrt{a_6}\right)erfc\left(\frac{y\sqrt{\mathrm{Pr}}}{2\sqrt{t}}-\sqrt{\frac{a_6 t}{\mathrm{Pr}}}\right)\end{array}\right]$$

 DOI : 10.35291/2454-9150.2019.0483

$$-\frac{A_8\,e^{(b_2t)}}{2}\begin{bmatrix}\exp\left(y\sqrt{b}\right)erfc\left(\frac{y\sqrt{\Pr}}{2\sqrt{\alpha t}}+\sqrt{\frac{bt}{\Pr}}\right)\\+\exp\left(-y\sqrt{b}\right)erfc\left(\frac{y\sqrt{\Pr}}{2\sqrt{\alpha t}}-\sqrt{\frac{bt}{\Pr}}\right)\end{bmatrix}$$

$$+\frac{A_9}{2}\begin{bmatrix}\exp\left(y\sqrt{kSc}\right)erfc\left(\frac{y\sqrt{Sc}}{2\sqrt{t}}+\sqrt{kt}\right)\\+\exp\left(-y\sqrt{kSc}\right)erfc\left(\frac{y\sqrt{Sc}}{2\sqrt{t}}-\sqrt{kt}\right)\end{bmatrix}$$

$$+A_{10}\begin{bmatrix}\left(\frac{t}{2}+\frac{y\sqrt{Sc}}{4\sqrt{k}}\right)\exp\left(y\sqrt{kSc}\right)erfc\left(\frac{y\sqrt{Sc}}{2\sqrt{t}}+\sqrt{kt}\right)\\+\left(\frac{t}{2}-\frac{y\sqrt{Sc}}{4\sqrt{k}}\right)\exp\left(-y\sqrt{kSc}\right)erfc\left(\frac{y\sqrt{Sc}}{2\sqrt{t}}-\sqrt{kt}\right)\end{bmatrix}$$

$$+\frac{A_{11}\,e^{(-b_{10}t)}}{2}\begin{bmatrix}\exp\left(y\sqrt{(k-b_{10})Sc}\right)erfc\left(\frac{y\sqrt{Sc}}{2\sqrt{t}}+\sqrt{(k-b_{10})t}\right)\\+\exp\left(-y\sqrt{(k-b_{10})Sc}\right)erfc\left(\frac{y\sqrt{Sc}}{2\sqrt{t}}-\sqrt{(k-b_{10})t}\right)\end{bmatrix}$$

$$+\frac{A_{12}\,e^{(b_2t)}}{2}\begin{bmatrix}\exp\left(y\sqrt{(k+b_2)Sc}\right)erfc\left(\frac{y\sqrt{Sc}}{2\sqrt{t}}+\sqrt{(k+b_2)t}\right)\\+\exp\left(-y\sqrt{(k+b_2)Sc}\right)erfc\left(\frac{y\sqrt{Sc}}{2\sqrt{t}}-\sqrt{(k+b_2)t}\right)\end{bmatrix} \quad (14)$$

where

$$\alpha=\frac{3R+4}{3R},\ B=\left(1+\frac{1}{\gamma}\right),\ a_1=\frac{N}{B},\ a_2=\frac{(N+a_0)}{B},$$

$$a_3=\frac{(N-b_8)}{B},\ a_4=\frac{(N-b_{10})}{B},\ a_5=\frac{(N+b_2)}{B},$$

$$a_6=\frac{(Q-b_8)}{\alpha},\ N=M+\frac{1}{K},\ b=\frac{(Q+b_2)}{\alpha},\ b=\frac{(Q+b_2)}{\alpha},$$

$$b_0=\frac{Q}{\alpha},\ b_1=\frac{Sc\,S_oQ}{(\Pr-Sc\alpha)},\ b_2=\frac{Q-kSc\alpha}{(\Pr-Sc\alpha)}\ b_{16}=\frac{b_7}{Bb_8^2}$$

$$b_3=\frac{PrSoSc}{\Pr-Sc\alpha},\ b_4=\frac{b_1}{b_2},\ b_5=\frac{b_1}{b_2^2},\ b_6=\frac{b_3}{b_2},\ b_7=\frac{-Gr\alpha B}{\Pr B-\alpha},$$

$$b_8=\frac{QB-N\alpha}{\Pr B-\alpha},\ b_9=\frac{-Gm(1+b_4)B}{ScB-1},\ b_{10}=\frac{kBSc-N}{BSc-1}$$

$$,\ b_{11}=\frac{-GmB(b_5+b_6)}{BSc-1},\ b_{12}=\frac{GmB(b_5+b_6)}{ScB-1},\ b_{17}=\frac{b_7}{Bb_8}$$

$$b_{13}=\frac{Gm\alpha Bb_4}{\Pr B-\alpha},\ b_{15}=\frac{Gm\alpha B(b_5+b_6)}{\Pr B-\alpha},\ b_{18}=\frac{b_8}{Bb_{10}^2},$$

$$b_{19}=\frac{b_8}{Bb_{10}},\ b_{20}=\frac{b_{11}}{Bb_{10}},\ b_{21}=\frac{b_{12}}{B(b_2+b_{10})},\ b_{22}=\frac{b_{13}}{Ba_8^2},$$

$$b_{23}=\frac{b_{13}}{Bb_8},\ b_{24}=\frac{b_{15}}{Bb_8},\ b_{25}=\frac{b_{15}}{B(b_2+b_8)},$$

$$A_0=\left(b_{16}+b_{18}+b_{22}-b_{24}\right),\ A_1=\left(-b_{17}-b_{19}-b_{23}\right),$$

$$A_2=\left(-b_{16}-b_{22}+b_{24}-b_{25}\right),\ A_3=\left(-b_{18}+b_{20}+b_{21}\right),$$

$$A_4=\left(-b_{21}+a_{25}\right),\ A_8=b_{25},\ A_{10}=b_9,\ A_{12}=b_{21}$$

$$A_7=\left(b_{16}+a_{22}-b_{24}+b_{25}\right),\ A_5=\left(-b_{16}-b_{22}+a_{24}\right),$$

$$A_6=\left(b_{17}+b_{23}\right),\ A_9=\left(-b_{18}+b_{20}\right),\ A_{11}=\left(b_{18}-b_{20}-b_{21}\right),$$

III. NUSSELT NUMBER

From temperature field, the Nusselt number which is given in nondimensional form as follows:

$$Nu=-\left[\frac{\partial\theta}{\partial y}\right]_{y=0} \quad (15)$$

From Eqs. (12) and (15), we get a Nusselt number as follows:

$$Nu=-\begin{bmatrix}t\sqrt{b_0}\,erf\sqrt{\frac{Qt}{\Pr}}-t\sqrt{\frac{\Pr}{\alpha\pi t}}\exp\left(-\frac{Qt}{\Pr}\right)\\+\frac{\Pr\alpha}{2\sqrt{b_0}}erf\sqrt{\frac{Qt}{\Pr}}\end{bmatrix} \quad (16)$$

IV. SHERWOOD NUMBER

From concentration field, Sherwood number which is given in non–dimensional form as follows

$$Sh=-\left[\frac{\partial C}{\partial y}\right]_{y=0} \quad (17)$$

From Eqs. (13) and (17) we get Sherwood number as follows:

$$Sh=-(1+b_4)\begin{bmatrix}-\exp(-kt)\sqrt{\frac{tSc}{\pi}}+t\sqrt{kSc}\,efr\left(\sqrt{kt}\right)\\+\frac{\sqrt{Sc}}{2\sqrt{k}}erf\left(\sqrt{kt}\right)\end{bmatrix}$$

$$-(b_5+b_6)\left[-\exp(-kt)\sqrt{\frac{Sc}{\pi t}}+\sqrt{kSc}\,erf\left(\sqrt{kt}\right)\right]$$

$$-(b_5+b_6)\,e^{(b_2t)}\begin{bmatrix}-\exp(-kt-b_2t)\sqrt{\frac{Sc}{\pi t}}\\+\sqrt{(k+b_2)Sc}\,erf\left(\sqrt{(k+b_2)t}\right)\end{bmatrix}$$

$$+b_4\begin{bmatrix}t\exp\left(-\frac{Qt}{\Pr}\right)\sqrt{\frac{\Pr}{\pi\alpha t}}-t\sqrt{b_0}\,erf\left(\frac{Qt}{\Pr}\right)\\-\frac{\Pr}{2\sqrt{b_0}}erf\left(\sqrt{\frac{tQ}{\Pr}}\right)\end{bmatrix}$$

$$+(b_5+b_6)\left[-\exp\left(-\frac{Qt}{\Pr}\right)\sqrt{\frac{\Pr}{\pi\alpha t}}+\sqrt{b_0}erf\left(\sqrt{\frac{Qt}{\Pr}}\right)\right]$$

$$-(b_5+b_6)\,e^{(b_2t)}\begin{bmatrix}-\exp\left(-\frac{bt}{\Pr}\right)\sqrt{\frac{\Pr}{\pi\alpha t}}\\+\sqrt{b}\,erf\left(\sqrt{\frac{bt}{\Pr}}\right)\end{bmatrix} \quad (18)$$

V. RESULTS AND DISCUSSION

The equations (8)-(10) with the boundary condition (11) were solved analytically using the Laplace transform technique. The impacts of various governing dimensionless parameters are examined, namely the magnetic parameter (*M*), Casson parameter (γ), radiation parameter (*R*), heat source (*Q*), Schmidt parameter (*Sc*), Prandtl number (*Pr*), Soret number (*So*), thermal Grashof number (*Gr*), mass Grashof number (*Gm*) on the velocity, temperature,

 DOI : 10.35291/2454-9150.2019.0483

concentration, the rate of heat transfer and the rate of mass transfer are studied graphically shown in Figs. 2-17.

The effect of various flow parameters on the fluid temperature appears in Figs. 2-4. From Fig. 2 shows that the temperature decreases with the increasing values of Prandtl number. This is due to fact that an increment in Prandtl number fluid has a comparatively low thermal conductivity which reduces conduction and thereby thermal boundary layer thickness and as a result, temperature decreases. The effect of the heat generation and heat absorption on the temperature field appears in Fig. 3 it is clear that the presence of heat generation within the boundary layer causes the energy level to increase and thus the temperature of the fluid increases in the vicinity of the plate. On another hand, the presence of heat absorption within the boundary layer produces the opposite effect and accordingly the temperature of the fluid decreases. The temperature profiles at a different time in the presence of heat absorption are shown in Fig. 4 it is observed that the temperature increases with increasing time. The reason is that the heat supplied from the plate is aiding with the heat generated in the boundary layer to increase the fluid temperature.

Species concentration profiles for various values of Soret effect *So*, Schmidt number *Sc* appear in Figs. 5 and 6. From Fig. 5 reveals that the concentration field due to variation in Schmidt number for the gasses hydrogen (*Sc*=0.22), water-vapour (*Sc*=0.60), ammonia (*Sc*=0.78), carbon dioxide (*Sc*= 0.96). It is observed that concentration field is arrived regularly for hydrogen and accrues for carbon dioxide in comparison to water vapour. Thus, water vapour can be used for maintaining concentration field and hydrogen can be used for maintaining good concentration field. An increasing in Schmidt number leads to decreases in the concentration boundary layer thickness. From Fig. 6 depicts the species concentration increases with the increasing values of *So*. These effects are much stronger near the surface of the plate. This indicates that the fluid species concentration rises due to greater thermal diffusion.

The velocity profiles for an oscillatory motion are presented from figures (7) to (13). The effects of *M*, γ, ω, *Sc*, *So*, *K* and *t* on the velocity field appear in Figs. (7) - (13). From Fig. 7 demonstrates that an increase in magnetic parameter the velocity decreases. It is due to the fact that the application of transverse magnetic field will result in a Lorentz force similar to drag force, which tends to resist the fluid flow and thus reducing its velocity profiles. The influence of Casson fluid parameter on velocity on profiles appears in Fig. 8 it is found that velocity increase with increasing values of Casson. It is consequential to note that an increment in Casson parameter makes the velocity boundary layer thickness shorter. It is further observed from this diagram when the Casson parameter is large enough, the non-Newtonian behaviors disappear and the fluid absolutely carries on like a Newtonian fluid. Subsequently, the velocity boundary layer thickness for Casson fluid is larger than the Newtonian fluid. It happens as a result of the plasticity of Casson fluid. At the point when Casson parameter diminishes the plasticity of the fluid increases, which causes the increment in velocity boundary layer thickness. From Fig. 9 it is observed that the fluid is oscillating between -1 and 1. These fluctuations near the plate are maximum and decrement for further values of independent variable *y*. This figure can facilely avail us to check the accuracy of our results. For reveals that the results we have concentrated more on the values of $\omega t = 0, \pi/2,$ and π. We can see optically discriminate that for these values of, the velocity shows its value either 1, 0 or -1 which are identical with the imposed boundary conditions of velocity in equation (12). Hence, both the graphical and scientific results are found in excellent agreement. In Fig. 10 depicts that the velocity increases with the increasing values of *K*. From Fig. 11 we observed that the velocity increases with an increasing value of *Sc*. Due to fact that the Schmidt number is dependent on mass diffusion and an increase in Schmidt number corresponds to an increasing mass diffusion and the velocity profile reduced. From Fig. 12 illustrate that the velocity decreases with increasing values of *So*. This implies that the generated thermal buoyancy and concentration buoyancy force leads to accelerating the fluid particles in the flow direction. The effects of *t* on the velocity field are shown in Fig. 13 reveals that the velocity increases with an increasing value of *t*. This is because an increase in *t* leads to an increase in the buoyancy force which causes an increase in the fluid velocity.

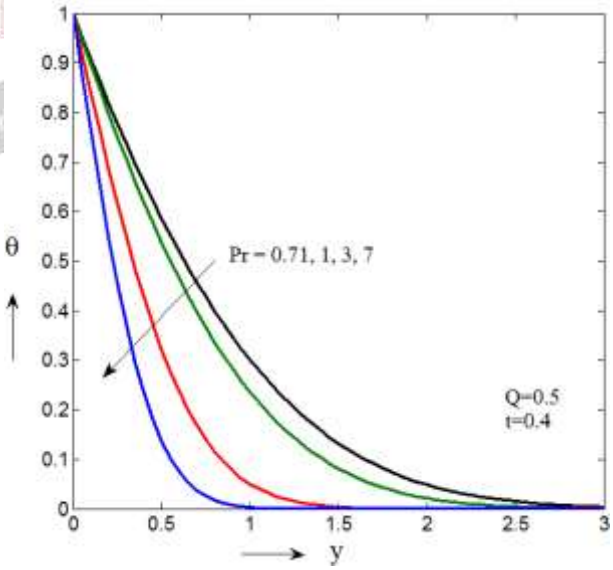

Fig. 2 Effect of Prandtl number on temperature

 DOI : 10.35291/2454-9150.2019.0483

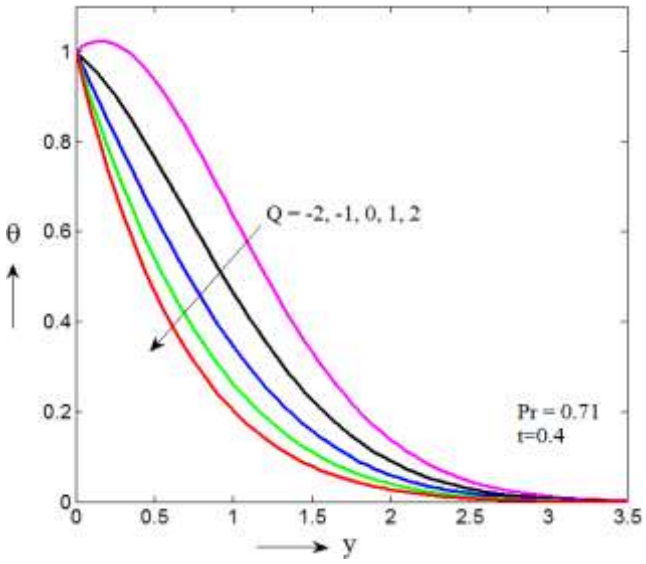

Fig. 3 Effect of heat source on temperature

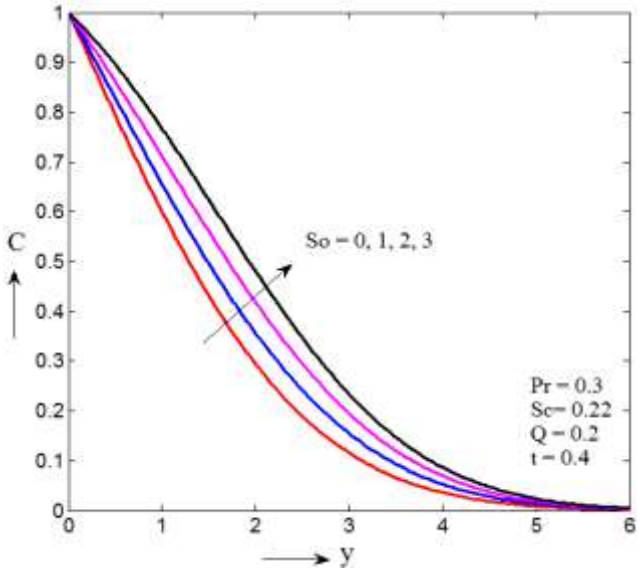

Fig. 6 Effect of Soret effect on concentration

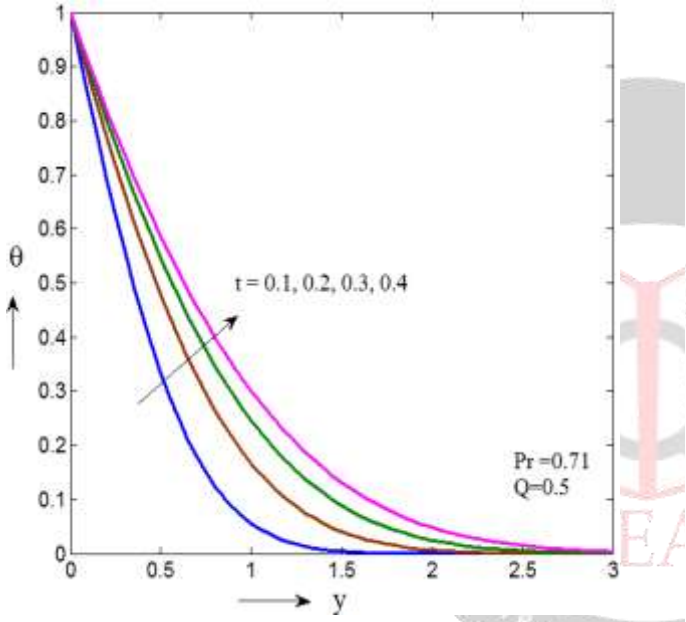

Fig. 4 Effect of time on temperature

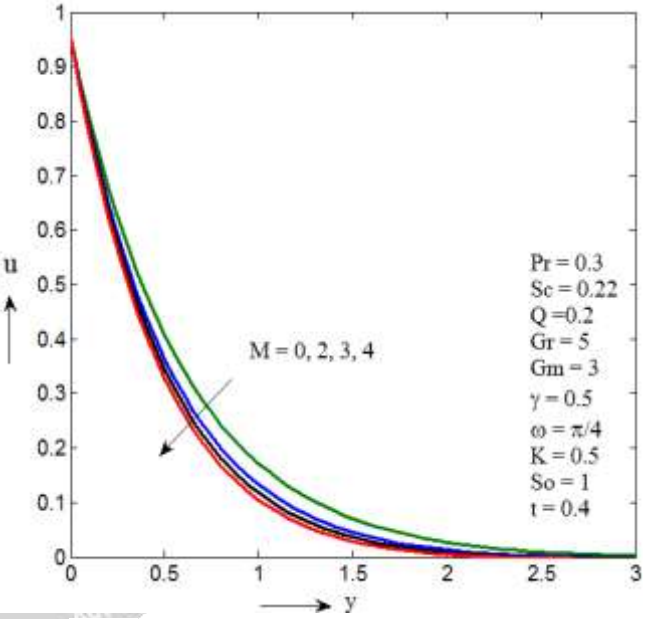

Fig. 7 Effect of magnetic parameter on velocity

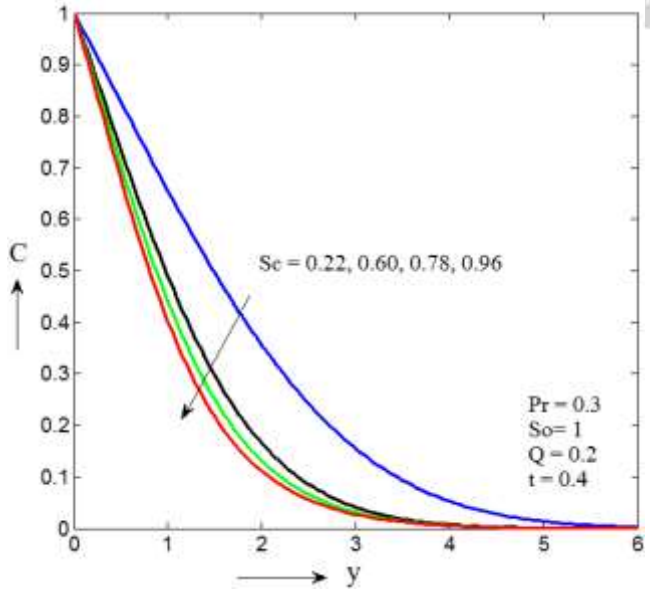

Fig. 5 Effect of Schmidt number on concentration

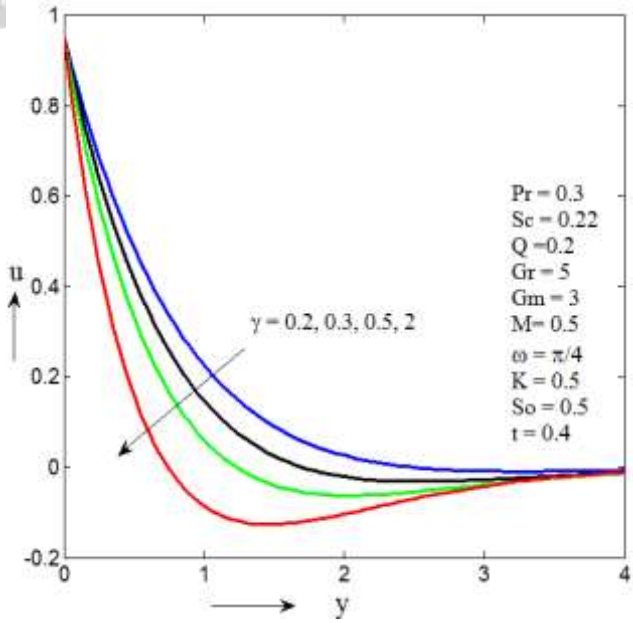

Fig. 8 Effect of Casson parameter on velocity

 DOI : 10.35291/2454-9150.2019.0483

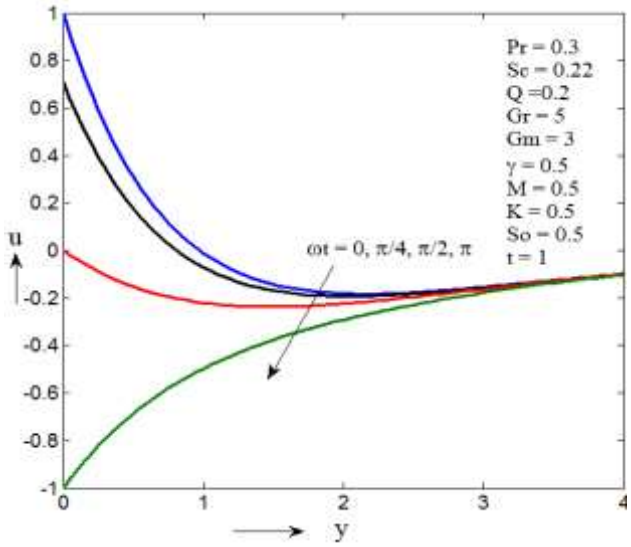

Fig. 9 Effect of ωt on velocity

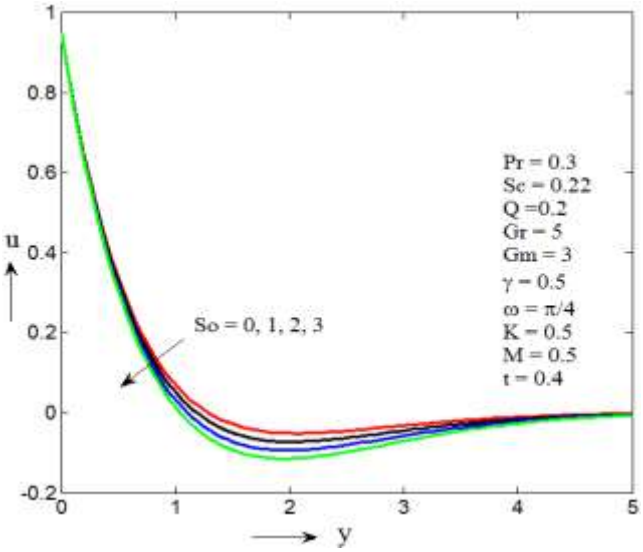

Fig. 12 Effect of Soret effect on velocity

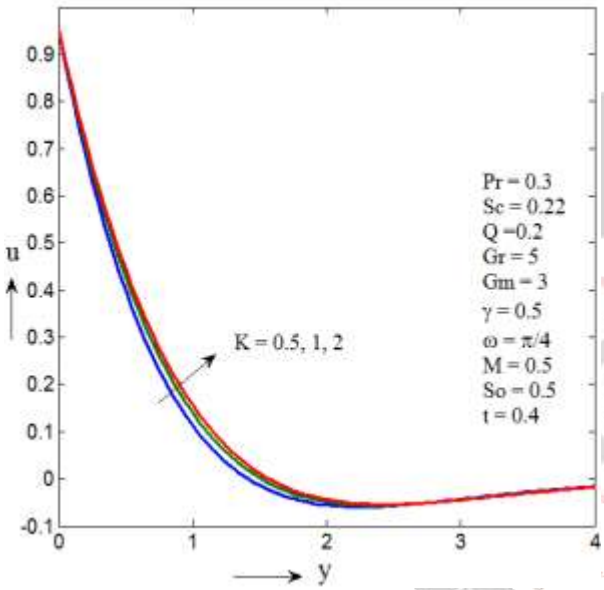

Fig. 10 Effect of *K* on velocity

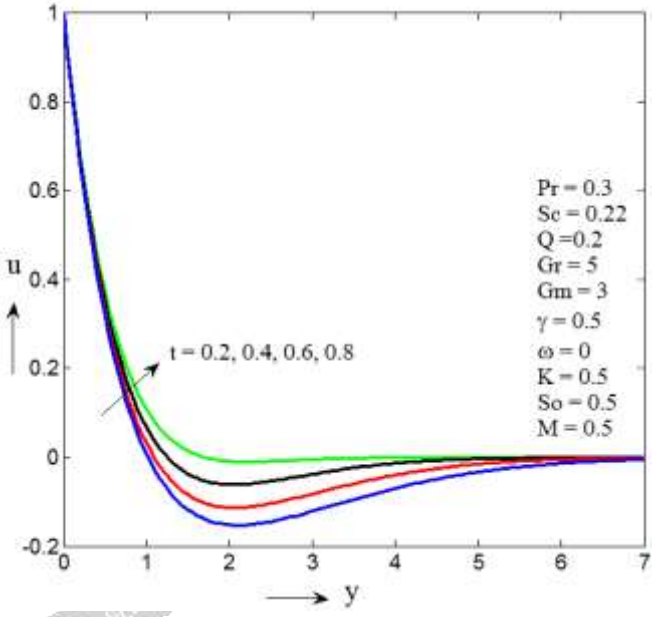

Fig. 13 Effect of time on velocity

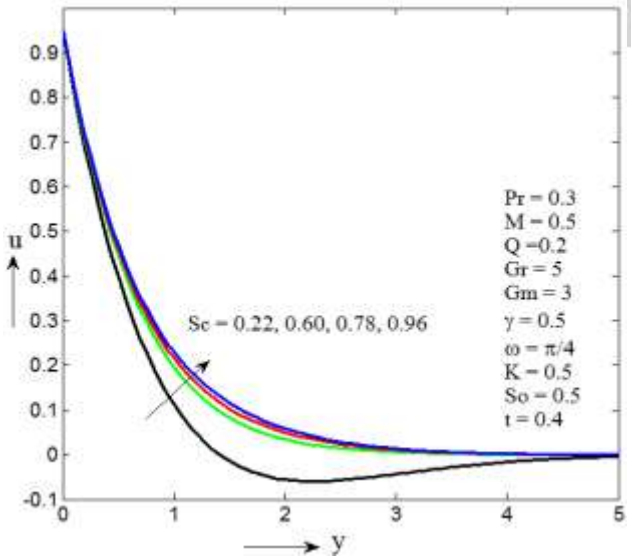

Fig. 11 Effect of Schmidt number on velocity

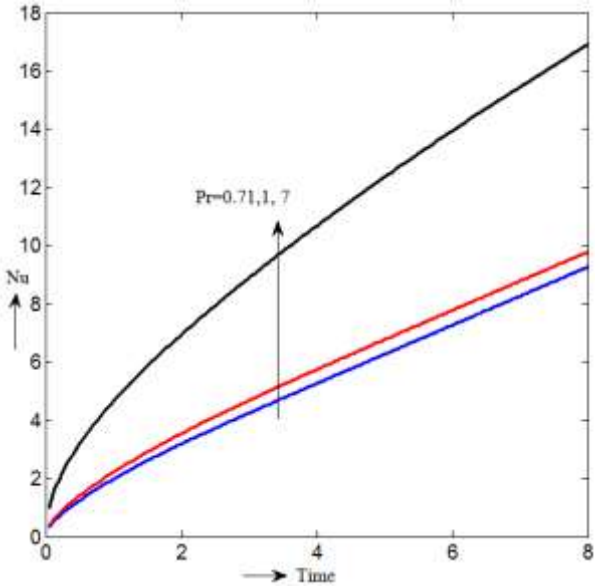

Fig. 14 Effect of Pr on Nusselt number

 DOI : 10.35291/2454-9150.2019.0483

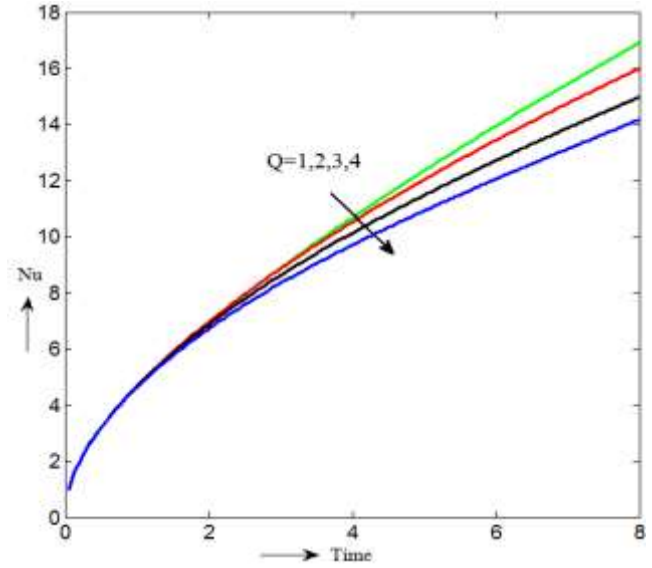

Fig. 15 Effect of Q on Nusselt number

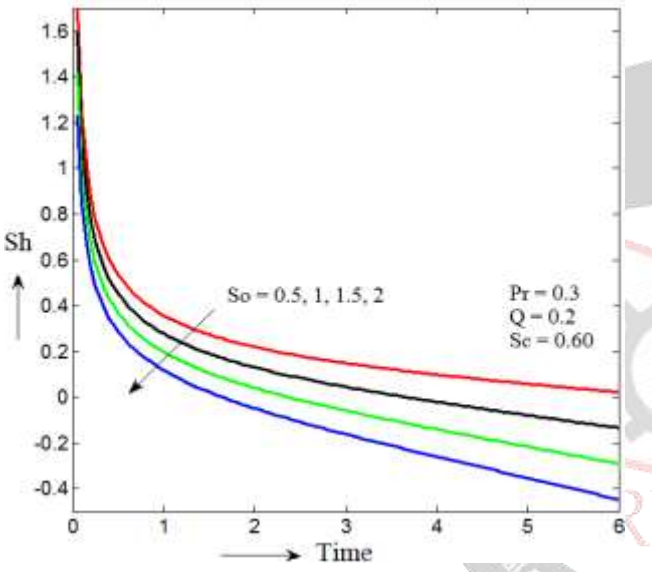

Fig. 16 Effect of *So* on Sherwood number

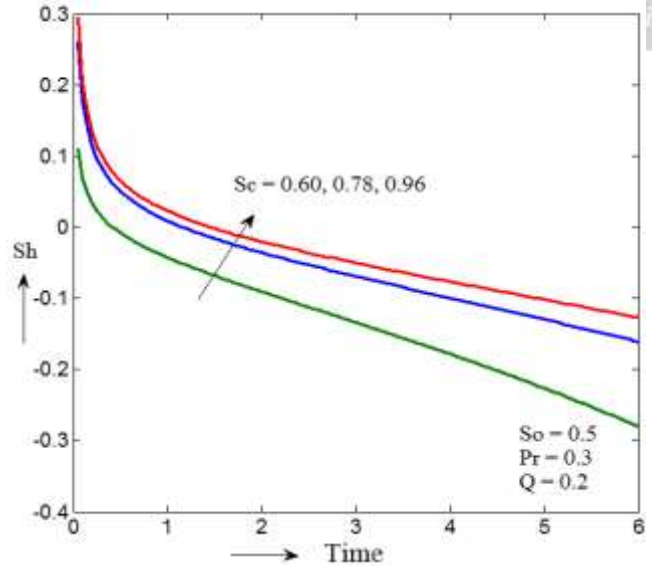

Fig. 17 Effect of *Sc* on Sherwood number

From Fig. 14 demonstrates that the Nusselt number against time *t*. The Nusselt number increases with increasing values of *Pr* for both air and water. It is also observed that the rate of change of heat transfer at the plate for water is higher than that of air. The reason is that lower values of *Pr* are equivalent to increasing the thermal conductivities and therefore, heat is able to spread out away from the plate more rapidly than higher values of *Pr*, since the rate of heat transfer is reduced. In Fig. 15 it is noticed that the Nusselt number decreases with different values of heat source parameter. In the case of heat absorption, the absorbed heat by the fluid causes to decrease of more number of energy levels. From Fig. 16 shows that the Sherwood number against time *t*. It is noticed that the rate of mass transfer at the plate decreases with increasing of *So*. This is attributed due to the concentration boundary thickness is high and as a result, the rate of mass transfer reduce. In Fig. 17 illustrate that the Sherwood number increases with increasing values of Sc.

VI. CONCLUSIONS

The study presented in this analysis of heat and mass transfer effects on unsteady MHD free convective Casson fluid flow past an oscillating semi-infinite vertical plate in the presence of a porous medium. The coupled linear governing equations were solved using the Laplace transform technique. Increasing the magnetic parameter decreases velocity profiles. Increasing the Casson parameter decreases the velocity profiles. The presence of heat source parameter does not seem to significantly change the results obtained by [11], the main difference is noted in the presence of Schmidt number and Soret effect parameters which they did not study. In this study, it is noted that increasing the Schmidt number decreases the species concentration profiles and species concentration increases with the increasing values of *So*.

Casson parameter diminishes the plasticity of the fluid increases, which causes the increment in velocity boundary layer thickness.

The temperature decreases with the increasing values of Prandtl number. This is due to fact that an increment in Prandtl number fluid has a comparatively low thermal conductivity which reduces conduction and thereby thermal boundary layer thickness and as a result, temperature decreases.

Thermal buoyancy and concentration buoyancy force leads to accelerating the fluid particles in the flow direction.

The Nusselt number increases with increasing values of *Pr* for both air and water. It is also observed that the rate of change of heat transfer at the plate for water is higher than that of air.

That the rate of mass transfer at the plate decreases with increasing of *So*. This is attributed due to the concentration boundary thickness is high and as a result, the rate of mass transfer reduces.

 DOI : 10.35291/2454-9150.2019.0483

ACKNOWLEDGMENT

The authors of the paper are thankful to the reviewers on their suggestions, which are significantly improved the quality of the paper.

REFERENCES

[1] L. Animasaun, Effects of thermophoresis, variable viscosity and thermal conductivity on free convective heat and mass transfer of non-Darcian MHD dissipative Casson fluid flow with suction and n^{th} order of chemical reaction, J. Nigerian Math Soci. 34 (2015)11–31.

[2] K. Bhattacharyya, Boundary layer stagnation-point flow of Casson fluid and heat transfer towards a shrinking/stretching sheet, FHMT. 4(2) (2013) 1-9.

[3] K. Bhattacharyya, T. Hayat, A. Alsaedi, Exact solution for boundary layer flow of Casson fluid over a permeable stretching/shrinking sheet, J. App. Math. Mech. 10, (2013) 1-7.

[4] J. Boyd, J.M. Buick, S. Green, Analysis of the Casson and Carreau-Yasuda non- Newtonian blood models in steady and oscillatory flow using the lattice Boltzmann method, Phys. Fluids 19 (9) (2007) 093103.

[5] N. Casson, A flow equation for the pigment oil suspensions of the printing ink type, in: Rheology of Disperse Systems, Pergamon, New York. (1959) 84-102.

[6] R.K. Dash, K.N. Mehta, G. Jayaraman, Casson fluid flow in a pipe filled with a homogeneous porous medium, Int. J. Eng. Sci. 34(10) (1996) 1145–1156.

[7] M.A. Emmanuel, I. Yakubu Seini, L. Bortey Bortteir, Analysis of Casson fluid flow over a vertical porous surface with chemical reaction in the presence of magnetic field, J. App. Math. Phys. 3(6) (2015) 713 - 723.

[8] R.K. Hari, H.R. Patel, Radiation and chemical reaction effects on MHD Casson fluid flow past an oscillating vertical plate embedded in the porous medium, Alexandria Eng. J. 55(1) (2016) 583-595.

[9] T. Hayat, S.A. Shehzad, A. Alsaedi, M.S. Alhothuali, Mixed convection stagnation point flow of Casson fluid with the convective boundary condition, Chin. Phys. Lett. 29 (2012) 114704.

[10] T. Hayat, S.A. Shehzadi, A. Alsaedi, Soret and Dufour effects on magneto hydrodynamic (MHD) flow of Casson fluid. App. Math. Mech. 33 (2012)1301–1312.

[11] A. Khalid, I. Khan, A. Khan, S. Shafie, Unsteady MHD free convection flow of Casson fluid past over an oscillating vertical plate embedded in a porous medium, Eng. Sci. and Tech., an Int. J. 18(3) (2015) 309 -317.

[12] I. Khan, F. Ali, S. Shafie, M. Qasim, Unsteady free convection flow in a Walters'-B fluid and heat transfer analysis. Bull. Malays. Math. Sci. Soc. 37 (2014) 437-448.

[13] F. Mabood, W. A. Khan, A. I. M. Ismail, Multiple slips effects on MHD Casson fluid flow in porous medium with radiation and chemical reaction, Can. J. Phys. 94(1) (2016) 26-34.

[14] S. Mukhopadhyay, K. Vajravelu, Diffusion of chemically reactive species in Casson fluid flow over an unsteady permeable stretching surface, J. Hydrodynamics **25** (2013) 591-598.

[15] V. Mernonr, J.N. Mazumdar, S. K. Lucas, A mathematical study of peristaltic transport of a Casson fluid, Math. Comp. Modell. 35, (2002) 895-912.

[16] M. Mustafa, T. Hayat, I. Pop, A. Aziz, Unsteady boundary layer flow of a Casson fluid due to an impulsively started moving the flat plate, Heat Transfer-Asian Res. 40 (2011) 563–576.

[17] M. Mustafa, T. Hayat, I. Pop, A.A. Hendi, Stagnation-point flow and heat transfer of a Casson fluid towards a stretching sheet, Z. Naturforschung 67(1-2) (2012) 1-7.

[18] S. Nadeem, R.U. Haq, C. Lee, MHD flow of a Casson fluid over an exponentially shrinking sheet, Scientia Iranica 19 (2012) 1550–1553.

[19] S. Pramanik, Casson fluid flow and heat transfer past an exponentially porous stretching surface in presence of thermal radiation, Ain Shams Eng. J. 5(1) (2014) 205-212.

[20] B. Rushi Kumar, T. Sravan Kumar and A.G. Vijaya Kumar, Thermal diffusion and radiation effects on unsteady free convection flow in the presence of magnetic field fixed relative to the fluid or to the plate, FHMT 6 (2015) 6-12.

[21] S.A. Shehzad, T. Hayat, M. Qasim, S. Asghar, Effects of mass transfer on the MHD flow of Casson fluid with chemical reaction and suction, Braz. J. Chem. Eng. 30(1) (2013)187-195.

[22] J.V.R. Reddy, V. Sugunamma, N. Sandeep Effect of aligned magnetic field on Casson fluid flow past a vertical oscillating plate in a porous medium. J.Adv. Phys. 5(4) (2016) 295-301.

[23] R.P. Sharma, K. Avinash, N. Sandeep, O.D. Makinde, Thermal radiation effect on non-Newtonian fluid flow over a stretched sheet of non-uniform thickness. Def. Diff. Forum 377 (2017) 242-259.

[24] J.V.R. Reddy, V. Sugunamma, N. Sandeep, P.M. Krishna, Thermal diffusion and chemical reaction effects on unsteady MHD dusty viscous flow. Adv. Phys. Theor. Appl. 38 (2015) 7-21.

[25] J.V.R. Reddy, V. Sugunamma, N. Sandeep, C. Sulochana, Influence of chemical reaction, radiation and rotation on MHD nanofluid flow past a permeable flat plate in porous medium. J. Nigerian Math. Soc. 35(1) (2016) 48-65.

[26] M. Swati, Casson fluid flow and heat transfer over a nonlinearly stretching surface, Chin. Phys. 22(7) (2013) 074701.

[27] K. Vajravelu, S. Mukhopadhyay, Diffusion of chemically reactive species in Casson fluid flow over an unsteady permeable stretching surface, J. Hydrodynamics, Ser. B **25**, (2013) 591-598.

[28] Veera Reddy, GSS Raju and A.G. Vijaya Kumar. Heat and mass transfer effects on unsteady MHD Casson fluid past a vertical plate in the presence of porous

 DOI : 10.35291/2454-9150.2019.0483

medium, Indian Journal of Applied Research, Vol. 9, Issue 5 (2019), 1-5.

NOMENCLATURE

B_0 External magnetic field (A.m^2)
C' Species concentration
C'_w Concentration of the plate
C'_∞ Concentration of the fluid far away from the plate
C Dimensionless concentration(kg/m^3)
C_p Specific heat at constant pressure(J/kg.K)
g Acceleration due to gravity (m/s^2)
K Porous medium
Gr Thermal Grashof number
Gm Mass Grashof number
M Magnetic field parameter(Am^{-1})
Pr Prandtl number
Q Heat source parameter
Sc Schmidt number
T' Temperature of the fluid near the plate(K)
T'_w Temperature of the plate
T'_∞ Temperature of the fluid far away from from the plate

t Dimensionless time (Sec)
u' Velocity of the fluid in the y' - direction
u_0 Velocity of the plate
u Dimensionless velocity(ms^{-1})
y' Co-ordinate axis normal to the plate

Greek symbols

β Volumetric coefficient of thermal expansion
β^* Volumetric coefficient of expansion with concentration
ωt Phase angle
μ Coefficient of viscosity (m^{2}s^{-1})
γ Casson fluid
ν Kinematic viscosity (m^{2}s^{-1})
ρ Density of the fluid(kgm^{-3})
σ Electric conductivity(Sm^{-1})
θ Dimensionless temperature(K)

Subscripts

w Conditions on the wall
∞ Free stream conditions

 DOI : 10.35291/2454-9150.2019.0483